ORIGINAL PAPER

Ligand accessibility to heme cytochrome b_5 coordinating sphere and enzymatic activity enhancement upon tyrosine ionization

Alejandro K. Samhan-Arias[1] · Cristina M. Cordas[1] · Marta S. Carepo[1] · Luisa B. Maia[1] · Carlos Gutierrez-Merino[2] · Isabel Moura[1] · José J. G. Moura[1]

Abstract

Recently, we observed that at extreme alkaline pH, cytochrome b_5 (Cb_5) acquires a peroxidase-like activity upon formation of a low spin hemichrome associated with a non-native state. A functional characterization of Cb_5, in a wide pH range, shows that oxygenase/peroxidase activities are stimulated in alkaline media, and a correlation between tyrosine ionization and the attained enzymatic activities was noticed, associated with an altered heme spin state, when compared to acidic pH values at which the heme group is released. In these conditions, a competitive assay between imidazole binding and Cb_5 endogenous heme ligands revealed the appearance of a binding site for this exogenous ligand that promotes a heme group exposure to the solvent upon ligation. Our results shed light on the mechanism behind Cb_5 oxygenase/peroxidase activity stimulation in alkaline media and reveal a role of tyrosinate anion enhancing Cb_5 enzymatic activities on the distorted protein before maximum protein unfolding.

Abbreviations

Cb_5	Cytochrome b_5
CD	Circular dichroism
CV	Cyclic voltammetry
DTPA	Diethylenetriaminepentaacetic acid
D_2O	Deuterium oxide
EDTA	Ethylenediaminetetraacetic acid
EPR	Electron paramagnetic resonance
GDN	Guanidine chloride
H_2O_2	Hydrogen peroxide
NHE	Hydrogen electrode scale
NMR	Nuclear magnetic resonance

✉ Alejandro K. Samhan-Arias
  aksamhan@unex.es

✉ José J. G. Moura
  jjgm@fct.unl.pt

1 LAQV, REQUIMTE, Departamento de Química, Faculdade de Ciências e Tecnologia, Universidade Nova de Lisboa, 2829-516 Lisbon, Portugal

2 Department of Biochemistry and Molecular Biology, Faculty of Sciences and Institute of Molecular Pathology Biomarkers, University of Extremadura, 06006 Badajoz, Spain

Introduction

Oxidation is the most common event associated with loss of hemoprotein function. The most typical example is the case of hemoglobin where methemoglobin, the oxidized form of hemoglobin, is unable to bind oxygen. Hemoprotein autoxidation process occurs naturally in vivo and it is estimated that 1.9–3.8% of the hemoglobin found in blood is in the methemoglobin form, although higher percentages can be found in children [1]. Several causes have been related to hemoprotein oxidation, including genetic diseases, drug administration and oxidative stress [2, 3]. The ferric hexacoordinated aqueous states, in equilibria with the hydroxy form, are the most common states found in the hemoglobin superfamily during oxidation [4], although other forms of this protein have also been detected [5]. In metalloproteins, ligand accessibility to the metal is required for acquisition of enzymatic activities, although protein hemichromes (hemoproteins with conformational changes not implicating unfolding and alteration of heme coordination) present enzymatic activities [6–8]. In hemoglobin, a reversible

hemichrome type called hemichrome H was thought to represent the imidazole ligation to the heme group, with water displaced and capable of renaturing to functional hemoglobin [9]. Upon incubation with time, hemichrome H can be transformed to hemichrome B, which is incapable to renature into functional hemoglobin [5]. The electron paramagnetic resonance (EPR) parameters (g values) of the hemoglobin's hemichrome B were similar to those found for Cb_5 [10] and the hemichrome H had g values similar to those present upon addition of base to the *bis*-imidazole heme complex or to Cb_5 [11, 12].

Due to the presence of hemichromes in vivo (i.e., cold-water fishes, where different hemichrome types of hemoglobin have been reported), a biological relevance of these states has been suggested [13].

The interaction of ligands with Cb_5 has been overlooked for years due to its full coordination sphere. The non-covalently bound heme group of Cb_5 at neutral pH is bound to two histidine residues, in the fifth and sixth position, and therefore the protein is an electron carrier, member of the heme b-type hemoprotein family. Some early studies with Cb_5 showed that this protein can acquire a high spin state after protonation and deprotonation [11, 12, 14]. In addition, mutations of the Cb_5 coordinating histidines allowed the binding of other ligands such as CN^-, CO and O_2 to the hemoprotein [15, 16]. Very recently, we have found that at extreme alkaline pH values (pH 12), Cb_5 acquires a peroxidase-like activity upon formation of a low spin hemichrome associated with a non-native state [7]. This hexacoordinated hemichrome is characterized by a time dependent loss of the Soret band, a lower redox potential than the one found at neutral pH, associated with a more oxidized state of the protein, and the non increasing of the tryptophan fluorescence is indicative of the folded state mantainance. The hemichrome spin state can monitor the protein transition conformation between hexa- and pentacoordinated states, with an accessibility for exogenous ligands, when the protein is in this conformation. Noteworthy, it is unknown whether hydroxide anion has a specific role in the conformation acquired at alkaline pH values. The pK_a of some amino acid residues in the alkaline range can be listed: lysine (pK_a less than 10.4 [17], arginine pK_a approximately 13.8 [18] and tyrosine 10.3–10.4 [19]. In addition, the fluorescence properties of tyrosine allow to easily determine the exact pK_a for this residue of each protein that can be modulated by a specific microenvironment [20].

In the present manuscript, changes induced by pH on heme Cb_5 were monitored by cyclic voltammetry (CV), nuclear magnetic resonance (NMR), electronic absorption, fluorescence, EPR and circular dichroism (CD) spectroscopies. A structure–function characterization of the protein allowed us to reveal a catalytic peroxidase/oxygenase activity of Cb_5 that accompanies the ionization of a putative nearby tyrosine. Remarkably, the peroxidase activity

is strongly dependent on the stable conformation found at alkaline pH that keeps the heme group bound to the peptide chain.

Materials and methods

Purification of recombinant human erythrocyte Cb_5

Purification of recombinant human erythrocyte Cb_5 was performed by overexpression of the protein using transformed BL21 (DE3)-derived strains of *E. coli* containing the recombinant plasmid as described before [21].

NMR

Samples were measured using 0.5 mM Cb_5 samples, in buffer + 10% D_2O. NMR spectroscopy experiments were carried out at 25 °C in a Bruker Avance II-600 spectrometer equipped with a TCI cryoprobe and a variable temperature control unit. The zgesgp pulse sequence was chosen, with a spectral width of 70 ppm, 64 k data points, and 1024 scans accumulated per spectrum. Experiments were carried out by adjusting the pH with the addition of small amounts of HCl or NaOH and monitored by a Crison micro pH 2002 pH meter equipped with a micro pH electrode (Cat #5209). All spectra were processed using TOPSPIN 3.2 (Bruker). Assignments for all four heme methyl groups, the 2-vinyl protons, two of the four propionate β-methylene protons and some amino acid side chains in the vicinity of pyrroles I and II have been reported previously [22, 23]. [1]H chemical shifts were referenced to the H_2O resonance (4.76 ppm at 298 K).

Fluorescence measurements

Tryptophan fluorescence of Cb_5 (5 μM) was measured using a fluorescence spectrophotometer (Perkin Elmer 650–40; Perkin Elmer, Norwalk, CT, USA) and quartz thermostated cuvettes (2 mL) at 25 °C. The excitation and emission wavelengths were 290 nm and 350 nm, respectively. The excitation and emission slits were 2 and 5 nm, respectively. The buffer used in the measurements was potassium phosphate 100 mM, borate 50 mM, KCl 150 mM, EDTA 1 mM prepared at different pH values, or GDN 10 M, under stirring. Tyrosine fluorescence of Cb_5 (5 μM) was measured with the same buffer conditions as used before at 25 °C. The fixed excitation and emission wavelengths were 270 nm and 305 nm. The excitation and emission slits were 2 and 4 nm, respectively.

Inner filter correction was applied to fluorescence data, as previously indicated [21, 24, 25]:

$$F_{corr} = F_{obs} * 10^{\left(\frac{Exc\ O.D. + Em\ O.D.}{2}\right)},$$

where F_{corr} and F_{obs} are the corrected and observed fluorescence, respectively, and Exc O.D. and Em O.D. are the sample optical densities at the excitation and emission wavelengths, respectively.

Electrochemistry

All measurements were performed at room temperature in anaerobic conditions (20 min of argon bubbling and keeping the electrochemical cell under positive argon atmosphere during the assays) as previously indicated [7]. The experiments were attained using a PGSTAT12 or a PGSTAT30 AUTOLAB potentiostat/galvanostat and analysis of the data was performed using GPES (Eco Chimie) software. The working electrode was a mercaptopropionic acid-modified gold disk, secondary electrode was a Pt wire and reference electrode was an Ag/AgCl electrode, in a single cell compartment. Proteins were immobilized using a membrane (3 kDa cutoff). CV assays were performed at different scan rates to define the best conditions to measure Cb_5 redox features and its pH dependence (5 mV/s^{-1}). Second scans of multiple assays (at least three replicates), performed at each pH value, were used for the analysis. All the potentials were converted and are presented in reference to the normal hydrogen electrode scale (NHE).

EPR measurements

The X-band EPR spectrum of Cb_5 at different pH values was measured as previously described [7], using a Bruker EMX 6/1 spectrometer and a dual mode ER4116DM rectangular cavity (Bruker); the samples were cooled with liquid helium in an Oxford Instruments ESR900 continuous-flow cryostat, fitted with a temperature controller. The spectra were acquired at 10 K, with a modulation frequency of 100 kHz, modulation amplitude of 0.5 mT and microwave power of 635 μW. The assay conditions are described in figure captions.

Oxygenase and peroxidase activity

Oxygenase and peroxidase activities were measured tracking the oxidation of Amplex Red [7], in the absence and presence of H_2O_2, respectively. Fluorescence was recorded using a spectrofluorimeter Perkin-Elmer 650-40 with the following setup: excitation and emission wavelengths of 530 nm and 590 nm, with excitation and emission slits of 5 and 10 nm and normal gain. Resorufin was used to calibrate the signal.

Imidazole binding analysis

Titrations with imidazole were performed after incubations of Cb_5 (50 μM) in a buffer with the following composition: phosphate buffer 100 mM, borate 50 mM, KCl 150 mM, EDTA 1 mM at the indicated pH for each experiment. Incubation times were selected based on Cb_5 Soret band stabilization kinetic present at each pH. After protein incubation, Cb_5 was diluted to 5 μM with buffer prepared at the same pH but supplemented with imidazole. Absorbance spectra were immediately recorded. The dissociation constant for the complex formation was calculated based on the Soret absorbance increase at 414 nm observed, when Cb_5 was added to the buffer in the presence of increasing imidazole concentrations. The analysis of imidazole binding to the protein was performed as indicated in [26]. Only imidazole is able to bind to the heme center in relationship to imidazolium and imidazolate that do not bind (pK_{a1} and pK_{a2} is 7.05 and 14.4, respectively) The calculated amount of imidazolate was approximately 1% at pH 13.5 and thus omitted in calculation of the free imidazole amount present at the measured alkaline pH values.

Circular dichroism measurements

Circular dichroism (CD) measurements were carried out in a Chirascan qCD spectrometer (Applied Photophysics) at 25 °C. The Cb_5 (16 μM or 50 μM) CD spectra were recorded from 350 to 500 nm (Soret region) or 190 to 260 nm (far-UV), using a quartz cell of 10 mm or 0.2 mm, respectively. Cb_5 concentration was 15 μM and the visible CD measurements were done at different pH values, 4, 7, 11, 11.5, 12 and 12.5 Cb_5. The CD spectra were recorded after protein incubation in buffers at different pH values, for the previously indicated times at which the Soret band absorbance was stabilized. The acquisition conditions were the following: step size: 1 nm, bandwidth: 1 nm, 3 scans. The protein was afterward incubated with imidazole (250 mM) at the same pH values and the CD spectra were acquired using the same experimental conditions.

Materials

All materials used to perform the experiments shown in this manuscript were analytical-grade commercial reagents.

Statistical analysis

All the results reported in this paper are the average ± standard error (SE) of triplicate experiments.

Results

Structural alterations of Cb_5 induced by pH

We assigned the following resonances for the heme group on the ^{1}H-NMR spectra by comparison with previously

published assignments of Cb_5 [22, 23]: 5-Me, 7 alpha-CH, 6 alpha-CH, 6′ alpha-CH, 3-Me and 1-Me, corresponding to the resonances found at 21.7, 18.8, 16.4, 15.4, 13.9 and 11.9 ppm, respectively, at pH 7.0 (Fig. 1a). We found a major contribution for only one of the two heme isomers described for Cb_5 (assignment of the resonances at 31.3 and 21.7 ppm, for the 3′-Me corresponding to the "minor" and the 5-Me of the "major" orientation, respectively) being in the range of previously described ratios (1:5) for this protein [27].

On the pH range between 6 and 10, only modest changes were found in accordance with the presence of a low spin Cb_5 at pH 7.0 [7, 27]. In addition, the one-dimensional NMR spectra of Cb_5 obtained at these pH values are typical for a well-folded protein. At alkaline and acid pH, a chemical shift dependence of the heme resonances upon pH was found. A decrease of the resonance intensities was revealed above pH 11, to almost disappear at pH 12. The residual intensities were only detectable when the same experiments were performed by increasing the transients' accumulation at pH 12 (Supp Fig S1). Therefore, at pH 12, we identified the following signals of the following Cb_5 heme resonances (peak $b = 21.89$ ppm that corresponds to 5-Me and peak $e = 12.02$ ppm that corresponds to 1-Me), also present in samples at pH 11 with some deviations. Noteworthy, we were not able to make an assignment in some cases due to resonance overlapping, in correlation with results described in the literature: peak $a = 28.12$ ppm that might correspond to 2α-vinyl or an 8-Me of Cb_5 minor isomer [28]; $c = 17.16$ ppm that might correspond to 7-α CH minor isomer or meso Hs as previously described [28]. Moreover, we also found a very weak signal ($d = 14.81$ ppm) that we can speculate to correspond to 3-Me and the undetermined * and *' at 20.5 ppm and 19.79 ppm. In addition, we did not find resonances above 35 ppm (up to 150 ppm) that might suggest formation of high spin species (Supp. Fig S1). At pH 6.0, we found a decrease in the signal intensity that correlated with a protein tendency to aggregate at pH values below 5.0 (Fig. 1a). Hence, the ^1H NMR spectra of Cb_5 reported at pH 4.5 are related to the percentage of Cb_5 present in solution (approximately, 50% at pH 4.5, based on the number of scans per spectrum needed to approximately acquire the same NMR spectrum obtained at pH 5.0).

The same behavior found for the oxidized form of Cb_5 was also found for the reduced form (Supp. Fig. S2). We made a tentative assignment of some of the resonanced of the human erythrocyte ferroCb_5 based on those described for the trypsin digested native bovine liver Cb_5 reduced with dithionite at pH 7.0 [29]; this sequence was previously shown to be identical to that of erythrocyte Cb_5 [30]. The signals found at 9.91 ppm and 9.71 ppm would mainly correlate with those of δ meso-H and β meso-H signals found for the major isomer of the native bovine liver ferroCb_5 at 9.88 ppm and 9.71 ppm, but also the δ meso-H and β

meso-H of the minor isomer attributed to the resonance at 9.71 ppm at pH 7.0 of the trypsin-digested bovine liver ferroCb_5 [29].

Our data show that below pH 7, the signal intensity of the ferroCb_5 heme resonances decreased with an aggregation and precipitation of the sample below pH 5. At alkaline pH values, we observed a decrease of the signal intensity of ferroCb_5 heme resonances above pH 9, with a lack of detection of these resonances above pH 12 (Supp. Fig. S2).

To further prove that the changes observed in samples incubated below pH 5.0 were associated with sample aggregation, we evaluated this phenomenon by measuring the light scattering of samples in a range of pH values (Fig. 1b). We found a time-dependent increase of the light scattering measured by fluorescence in samples incubated at pH 4.0, that was maximum after 5 min incubation (Fig. 1b, inlet), not found in samples incubated at the rest of the measured pH values (Fig. 1b).

HSQC experiments were also performed at pH 4.8, 7.0 and 11.6 with the ^{15}N-labeled protein, in the presence of 10% of D_2O (Fig. 1c). The obtained NMR spectra suggest different protein behaviors when samples are incubated at alkaline or acid pH values. The spectra obtained at pH 7.0 resemble that previously obtained for this protein at this pH [21]. A deterioration of Cb_5 HSQC spectra was observed at pH 11.6, manifested by a qualitative intensity decrease of some of the heme resonances. This effect correlated with that found for other proteins with a distorted conformation [31]. The sample spectra of Cb_5 incubated at pH 4.8 differs from that obtained at pH 11.6 and pH 7. The narrow distribution of the protein chemical resonances indicates that the protein started to get denatured, a behavior observed in the HSQC spectra of other proteins in this state [32–34].

Moreover, Cb_5 secondary structure changes upon alkaline pH were studied by far-UV CD (Fig. 1d). At pH 7.0 (black line), we obtained a typical far-UV CD spectrum for a mainly α-helix protein with two negative maximums at 206 and 220 nm, as also previously described [35]. A decrease of the 220 nm band was observed at pH 11 (green line), although the protein was still structurally ordered. At pH 12 (red line), the 220 nm band further decreases and a negative band at 202 nm appears showing that at this pH we have a more disordered form of the protein and the secondary structure is affected. A more pronounced change to that measured at pH 12 was observed for the sample incubated at pH 12.5 (pink line). HSQC and CD spectra clearly demonstrate the loss of the native conformation of Cb_5 at alkaline pH.

We also studied the effect of acidic pH values (pH less than 7) on Cb_5 by EPR spectroscopy, aiming to follow the heme spin state changes and to compare them with those described at alkaline pH values (red line) [7] (Fig. 1e). At pH 5.0 (black line), the Cb_5 spectrum shows a low spin signal ($S = 1/2$) identical to that described at pH 7.0 ($g_{1,2,3} = 3.05$,
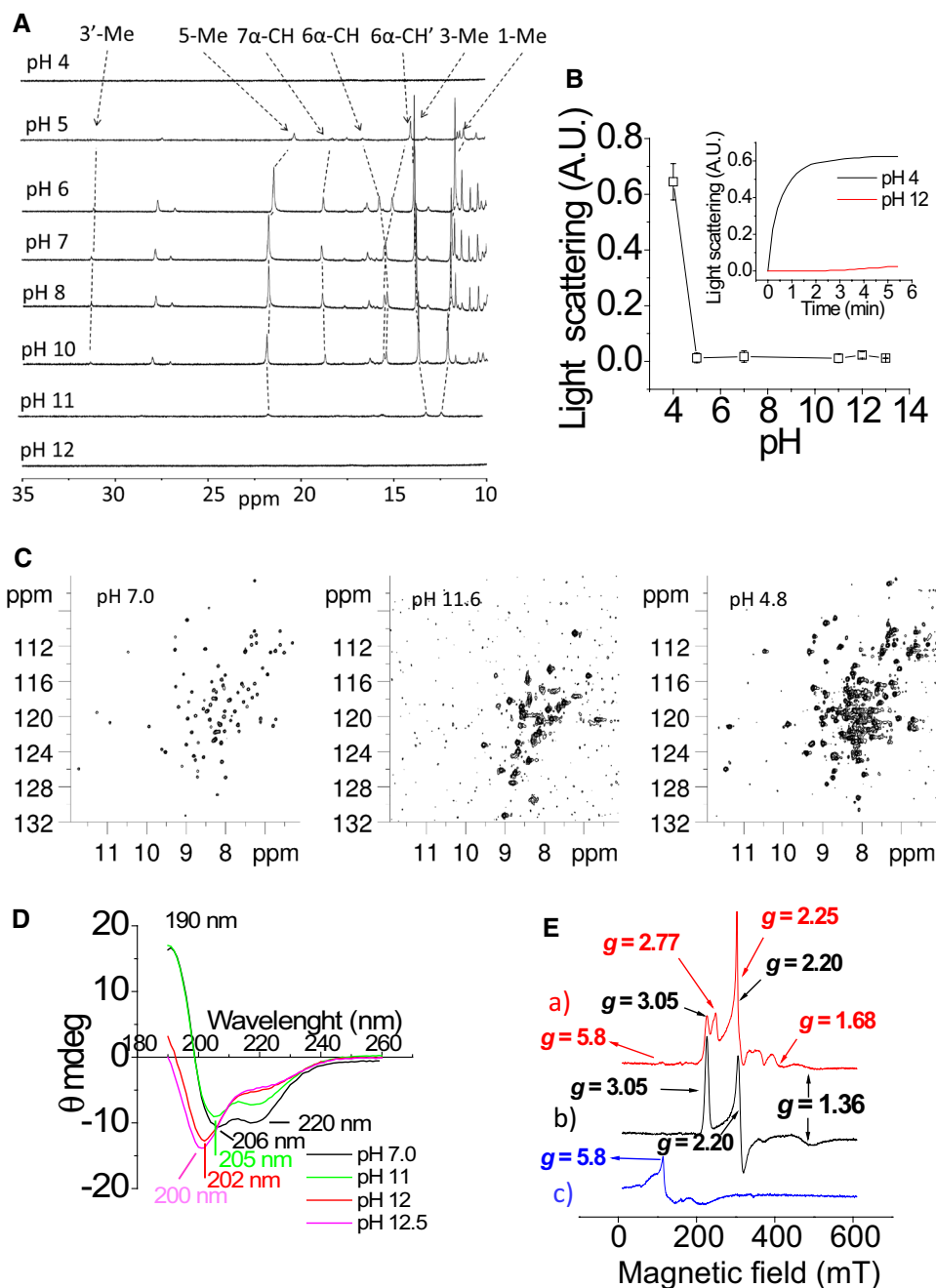
Fig. 1 ^{1}H-NMR spectra of Cb_5. ^{1}H-NMR spectra of Cb_5 acquired with a Bruker Avance operating at 600.13 MHz were measured using a solution of protein at 500 μM prepared in the following buffer: potassium phosphate 100 mM, borate 50 mM, KCl 100 mM, EDTA 1 mM 10% D_2O and measured using a 5 mm NMR tube. Samples were adjusted to the selected pH using a microelectrode before each measurement. **a** The Cb_5 spectra at the region from 35 to 10 ppm at pH 5.0, 6.0, 7.0, 8.0, 10.0, 11.0 and 12.0. **b** Light scattering measurements of Cb_5 incubated for 5 min in buffer prepared at different pH values using a Perkin-Elmer 650-40; PerkinElmer, Norwalk, CT, USA) using quartz cuvettes (2 mL) thermostated at 25 °C. The inlet shows the kinetics of the increase of light scattering of samples incubated at pH 4.0 (black line) vs. pH 12.0 (red line). **c** ^{15}N- and ^{1}H-HSQC spectra of Cb_5 (160 μM) in buffer at pH values: 7.0, 11.6 and 4.8. Spectra were acquired with ^{15}N-labeled protein in the pres-

ence of D_2O at 298 K using a Bruker Avance 600 MHz spectrometer equipped with a TCI cryoprobe. The 2D spectra were processed with TOPSPIN 2.1 (Bruker). The number of peaks counted over the background signal was 134, 57 and 134 for the samples incubated at pH 7, 11.6 and 4.8, respectively. **d**. Cb_5 far-UV CD spectra incubated at different pH values. Measurements were carried out in a Chirascan qCD spectrometer (Applied Photophysics) at 25 °C as indicated in "Materials and methods" and recorded from 190 to 260 nm, using a quartz cell of 0.2 mm. Cb_5 concentration was 50 μM and the measurements were performed at different pH values, 7 (black line), 11 (green line), 12 (dark blue line) and 12.5 (light blue line) at time 0. **e** Cb_5 EPR spectra at the X-band for samples incubated at pH 12.0 (red), 5.0 (black) and 4.0 (blue). The EPR spectra of Cb_5 incubated at pH 12.0 has been previously published [7]

2.20, 1.36 [7]). Yet, at pH 4.0 (Fig. 1e, blue line), the spectrum shows features characteristic of axial high spin ($S = 5/2$) Fe^{3+} species, with a main component at $g_\perp = 5.8$, for which a $g_{//}$ is approximately two is expected (not resolved). An intensity signal decrease of the Cb_5 EPR spectra sample incubated at pH 4.0, with respect to pH 5.0 and 12.0, could be associated with protein precipitation, as demonstrated by light scattering experiments.

Cb_5 oxygenase activity and correlation with redox potential

Activity measurements

Previous NMR and EPR experiments showed spin alterations on Cb_5 at acid (pH 4.0) and alkaline pH values (pH 12). The measurement of a free available coordination position on a protein can be used to foresee those conditions in which enzymatic activities can occur [36]. Since peroxidase and oxygenase activities share catalytic intermediaries in hemoproteins, oxygenase activity can be analyzed as a secondary activity present in proteins with peroxidase activity.

Measurement of the Amplex Red oxidation dependence upon pH, at a constant Cb_5 concentration (1 μM), allowed us to determine the pH values at which maximum oxygenase activity can be measured (Fig. 2a). A calibration curve with resorufin, the oxidation product of Amplex Red, at each pH allowed us to determine that the maximum oxygenase activity is reached at pH 4.0 and 13.5. At acid pH (pH 4.0), analysis of initial rates for Amplex Red oxidation (Fig. 2b, continuous line) allowed us to determine an oxygenase activity of 0.06 ± 0.01 nmoles/min/mg of Cb_5, although the activity was stopped after a couple of minutes (Fig. 2b, continuous line). Addition of Cb_5 to the buffers above pH 11.5 induced an increase on Amplex Red oxidation. After a lag phase of 1 min, an acceleration of the activity over time was detected (Fig. 2b, dotted line). The maximum measured oxygenase activity of Cb_5 was found at alkaline pH, in relationship to acidic values (at pH 13.5 the activity was 2.8 ± 0.2 nmoles/min/mg). Since the oxygenase activity measured at pH 12 (0.05 ± 0.01 nmoles/min/mg protein) was similar to that found at pH 4.0 (Table 1), we measured the peroxidase activity of Cb_5 at pH 4.0 (Fig. 2c) to compare with the values previously reported at pH 12 [7]. Addition of H_2O_2 to the sample (1 μM) induced a prominent increase on Amplex
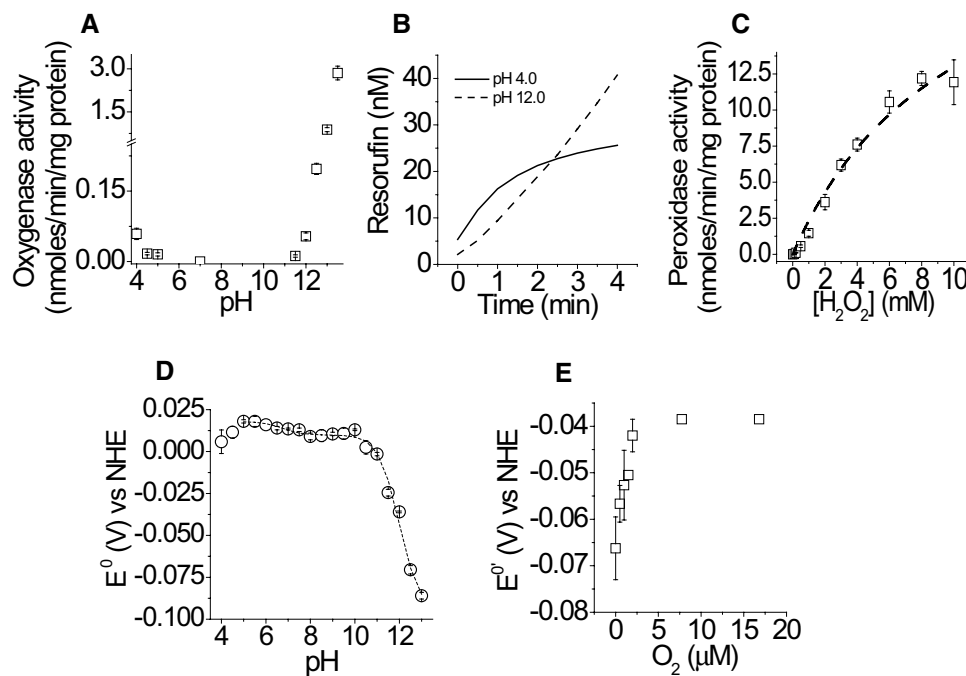
Fig. 2 Measurement of the oxygenase and peroxidase activity of Cb_5. Cb_5 oxygenase activity dependence upon pH (**a**). Cb_5 (1 μM) was incubated in buffers prepared at different pH values. Amplex Red oxidation was measured as indicated in "Materials and methods". The signal was calibrated at each pH with resorufin to obtain the values for the oxygenase activity. The kinetics for the oxygenase activity of Cb_5 at pH 4.0 (continuous line) and 13.0 (dashed line) is shown in **b**. The peroxidase activity of Cb_5 at pH 4.0 dependence with H_2O_2 is shown in **c**. Cb_5 formal redox potential vs. pH plot is shown in **d**. Plotting of the formal redox potential data vs. pH shows the large shift on the potential induced by incubation of Cb_5 in alkaline pH. Dashed gray line indicates the best data fitting considering two protonation processes. The effect of O_2 on Cb_5 redox potential at pH 12 is shown in **e**. A plot of the Cb_5 formal redox potential changes induced by O_2 is shown. The redox potential of Cb_5 was measured by CV at 5 mV/s scan rate in an anaerobic chamber

Red oxidation that was dependent upon H_2O_2 concentration. The curve was fitted to a two substrate Michaelis–Menten equation, considering Amplex Red and H_2O_2 as substrates [7], to obtain a k_{cat} value of 11 ± 1 ms^{-1} and a K_m for H_2O_2 of 12.3 ± 2.6 mM, for the peroxidase activity at pH 4. A summary of the reported activities of Cb_5, using Amplex Red as substrate can be found in Table 1. Although a correlation between activity and a negative shift on redox potential was previously shown [7], the complete redox potential changes sequence with the pH was also measured.

Redox potential measurement

Cb_5 redox behavior was evaluated by thin layer cyclic voltammetry in a pH range from 4.0 to 13.0. The representative Cb_5 voltammograms (with normalized current intensity after blank subtraction) obtained at different pH values are plotted in Fig. 2d (Supp. Figs. S3A, S3B and S3C show original voltammograms before subtraction and Supp. Fig. S3D after subtraction). The formal potential of Cb_5 suffers a small shift between pH 6 and 10, the formal potential increase being around 10 mV (Fig. 2d). The obtained pKox and pKred values are close, respectively, 6.7 ± 0.1 and 6.8 ± 0.1, and are similar to previously reported values by Lloyd et al. [27] (pKox and pKred of 6.0 ± 0.1 and 6.3 ± 0.1). However, due to its similarity (pKox approximately pKred), we must also consider the hypothesis that these values might not have physical meaning. When the redox potentials were measured in a wider pH scale range, we noticed that Cb_5 suffered a strong shift on the redox potential of around 90 mV from pH 10.0 to pH 13.0 (Fig. 2d). Below pH 5.5, we were also able to detect a smaller shift on its redox potential toward negative values, although we could not measure the changes associated with the whole transition since there are some limitations to measuring the redox potential below pH 4.0, i.e., loss of the current signal with respect to the controls. Fitting of the curve to a two pH-dependent equilibria allowed us to obtain the apparent pK_a values at alkaline conditions: pKox $= 11.6 \pm 0.1$ and pKred $= 12.3 \pm 0.1$. Since we cannot exclude that at alkaline pH Cb_5 conformational state may

be affected, (Fig. 2d), the pK values obtained at these pH ranges should be only considered as apparent pK values.

O_2 binding to Cb_5 at alkaline pH

A comparison of Cb_5 redox potential measurements performed under aerobic or anaerobic conditions allowed us to quantify a 30 mV difference on the protein formal potential between conditions. This difference may indicate O_2 binding to the protein center, associated with changes in the redox potential at pH 12. Cb_5 formal potential calculated from voltammograms obtained in strict anaerobic conditions, inside an anaerobic chamber, in the presence of non-deoxygenated water (oxygen concentration present in water was measured with an Oxygraph Plus DW1 electrode, Hansatech Instruments), suffered a concentration-dependent shift toward positive values (Fig. 2e). A shift of the formal potential with increasing amounts of O_2 was found, demonstrating the existence of protein interaction with the gas that may be binding to the heme group, since this ligation is expected to alter the center's formal potential [37, 38]. Plotting of Cb_5 formal redox potential values shifts upon different O_2 concentration exposition is shown in Supp. Fig. S3E. The data were fitted to a rectangular hyperbolic curve of the type: $y = P1*x/(P2 + x)$, where P1 is the number of binding sites (in our case, one center), x is the concentration of O_2 and P2 is equivalent to the equilibrium binding of the ligand to Cb_5. The solution of this equation gave us a K_d value of 1 ± 0.2 μM for the complex O_2:Cb_5.

Autofluorescence measurements

Tryptophan fluorescence

Tryptophan fluorescence was used to track structural changes on Cb_5 associated with its folding state (Fig. 3a). Addition of Cb_5 to the buffer at pH 4.0 (black line) revealed a kinetic process leading to an increase of the tryptophan fluorescence intensity in relationship to pH 7.0 (dashed line), with a half-life lower than 1 min, which correlated with the times where maximum oxygenase activity was shown at acid

Table 1 Enzymatic parameters of the peroxidase and oxygenase activity of Cb_5

Condition	Oxygenase activity (nmoles/min/mg protein)	Peroxidase activity (nmoles/min/mg protein)	K_d O_2 (μM)	K_m H_2O_2 (mM)	K_{cat} H_2O_2 (ms^{-1})
pH 4.0	0.06 ± 0.01	26 ± 5	N.D[a]	12.30 ± 2.60	11 ± 1
pH 12.0	0.05 ± 0.01	578 ± 41[b]	1[c]	0.95 ± 0.10[b]	700 ± 100[b]

[a]The small change observed in the Cb_5 redox potential did not allow us to accurately calculate the K_m for O_2 at acid pH

[b]Calculated from the previously obtained kinetic data [7]

[c]Apparent K_d based on cyclic voltammetry data

pH (Fig. 2b). An increase in the tryptophan autofluorescence was found above pH 12.1 (Fig. 3a and Supp. Fig. S4), with the rate of kinetic process being faster at pH values higher than 12.6, although reaching the same maximum fluorescence intensity between pH 12.6 and 13.2. Cb_5 fluorescence intensities found at acid and alkaline pH were lower than those obtained with GDN 6 M (red line), which contrasts with the intensity signal of the fully unfolded protein and points out that only a partial unfolding of Cb_5 is reached at pH values 4.0 and 12.6–13.2.

Tyrosine ionization

b_5 tyrosine fluorescence was measured as indicated in "Materials and methods". The fluorescence spectra of Cb_5 at pH 7.0 shows a maximum emission fluorescence band at 305 nm (black line) when an excitation wavelength at 270 nm was used (Fig. 3b). The same spectra measured at pH 12.0 show a decrease of the emission fluorescence intensity (arrow) that can be used to measure the pK_a of this residue, as calculated for other proteins [20]. The pK_a value of free tyrosine is known (10.3–10.4) [19]. Noteworthy, the pK_a value of the tyrosine residue in peptides and proteins can drastically shift depending on the microenvironment [20, 39–41]. The wavelengths at which Cb_5 shows the maximum fluorescence peak was monitored after addition of increasing concentrations of KOH (Fig. 3c). As shown in this figure, the results fit well with the Henderson–Hasselbalch equation and allow to calculate a pK_a of 11.1 ± 0.1.

Cb_5 absorption spectra at acid and alkaline pH

Cb_5 absorption was also studied over the pH. Cb_5 visible spectra were recorded from 350 nm to 750 nm wavelengths from pH 4.0 to 12.0. The protein remained stable with no changes on the visible spectra from pH 5 to 10. At acid pH (Fig. 4a) from 5.0 (blank line) to 4.0 (gray line), we found the existence of a fast transition on Cb_5 absorbance spectra. At pH 4.0, Cb_5 suffered a loss and shift of the Soret band at 413 nm to 407 nm and loss of the bands at 532 nm and 560 nm. We also found that these changes were paired with a slight absorbance intensity increase of bands located at 360–380 nm, 490–520 nm and 630–650 nm (Fig. 4a, inset graph). The appearance of these bands is indicative of acquisition of a high spin state by Cb_5 at this pH [12], but these bands are also similar to that found for free hemin. In addition, centrifugation of the sample at pH 4.0 during 15 min at 15,000g showed precipitation and formation of a red pellet, suggesting aggregates formation in the sample, or heme release to the media, as previously measured at acid pH when the apoprotein was prepared [42]. As previously shown, the spectral changes of Cb_5 incubated at alkaline pH can be easily monitored through its Soret band [7]. Cb_5 absorbance was tracked in time at 414 nm (Fig. 4b). An acceleration of the absorbance loss rate was observed when the protein was incubated at pH values above 11.0.
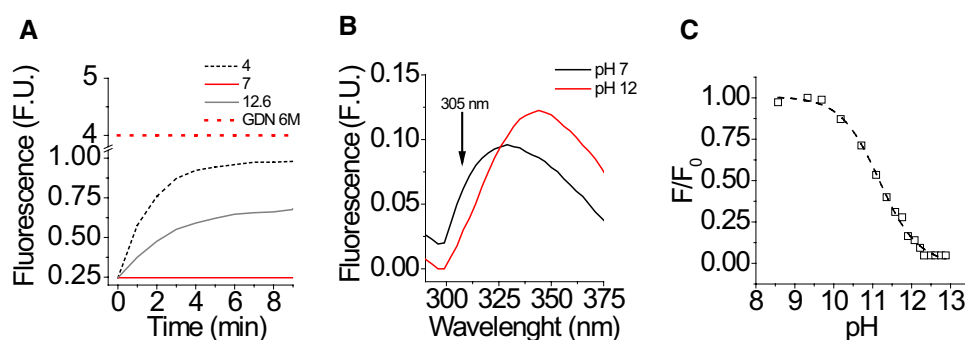
Fig. 3 Tryptophan and tyrosine fluorescence of Cb_5. Tryptophan fluorescence was measured as previously shown [7] and indicated in "Materials and methods" (**a**) at: pH 4.0 (dotted black line), 7.0 (continuous red line) and 12.6 (continuous gray line). The fluorescence intensity at each pH was compared to that obtained of Cb_5 in 6 M of guanidine chloride (GDN) (dotted red line). Emission spectra of Cb_5 prepared at pH 7.0 (black line) and pH 12.0 (gray line) with a tyrosine excitation wavelength of 270 nm are shown in **b**. Cb_5 fluorescence was measured as indicated in "Materials and methods" using a fluorescence spectrophotometer (Perkin-Elmer 650-40; PerkinElmer, Norwalk, CT, USA) using quartz thermostated cuvettes (2 mL) at 25 °C. The fixed excitation wavelength was 270 nm. The excitation and emission slits were 2 and 4 nm, respectively. Data intensities were normalized in this figure relative to the fluorescence intensity at pH 7.0 (F_0). Cb_5 tyrosine's fluorescence was titrated with pH with a fixed emission wavelength (305 nm) (**c**). Increasing amounts of concentrated NaOH were added to the cuvette to obtain a pK_a for tyrosine ionization

Fig. 4 Cb_5 electronic absorption spectra at acid and alkaline pH values. Cb_5 absorbance spectra (5 µM) was measured at pH 5.0 (black line) and 4.0 (gray line) **a**. The inlet figure shows a zoom of the 600–700 nm region for the sample incubated at pH 4.0, where a band at 635 nm rises. The kinetics of the Cb_5 Soret band absorbance loss (414 nm) of Cb_5 at pH 11.0 (black line), 11.5 (red line), 12.0 (blue line), 12.5 (pink line) and 13 (green line) is shown in **b**
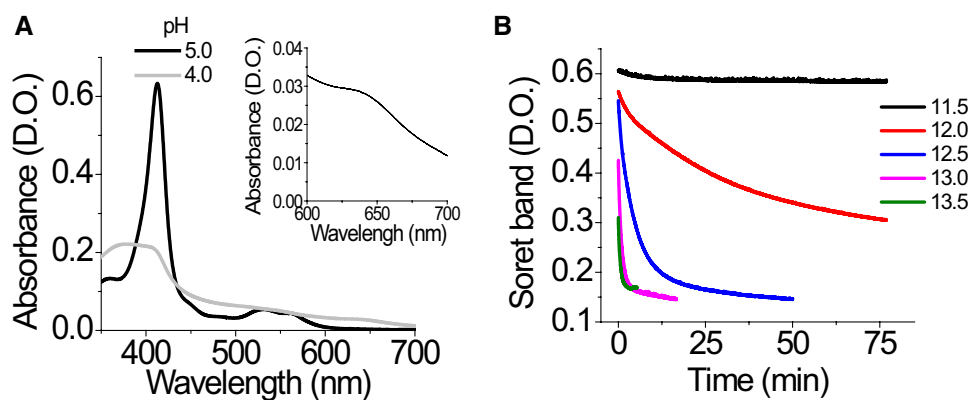
Heme binding properties to the peptide chain at different pH values

To further determine the ligation properties of the heme group to the protein, at different pH values where the Soret band was shown to disappear, Cb_5 (1 mL, 50 µM) aliquots prepared at different pH conditions were loaded onto a PD-10 (GE Healthcare) desalting chromatographic support (1 kDa exclusion limit) (Fig. 5). The protein (determined by the peak at 280 nm) was mainly eluted in fraction 5 at all measured pH values: 4.0, 7.0 and 12.6. A dependence of the Soret band intensity with pH was found. In addition, the band at 280 nm in fraction 5 (and the tail observed in

the following fractions) of the sample prepared at pH 4.0 was more intense than that found for the Soret band, suggesting that the heme group was released from the protein. At pH 12.6, we found a decrease of the Soret band with respect to the sample run at pH 7.0, but with a similar ratio between Soret and absorbance at 280 nm. In the sample previously incubated at pH 4.0, a fraction (32) was eluted from the column upon washing the column with NaOH, with maximum absorbance spectra at 392 nm (similar to the high spin heme) with a shoulder at 380 nm (similar to that of free heme). Non-spectral differences were found in the same fractions obtained at pH 7.0 and 12.6. Figure 5b
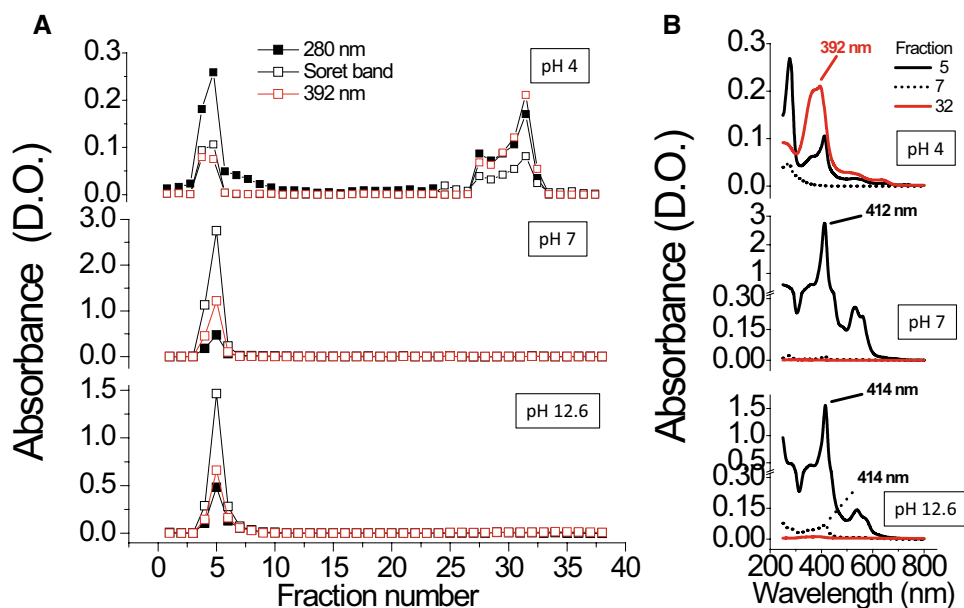
Fig. 5 Measurement of heme binding to the Cb_5 peptide chain at different pH values. Analysis of the heme binding properties to the peptide chain was performed by loading the protein incubated at different pH values: 4.0, 7.0 and 12.6 onto a PD10 column (8 mL) equilibrated at the same pH (**a**). After loading the sample, the column was washed with 15 mL of buffer and spectra of 1 mL aliquots were measured.

After washing the column with 10 mL of water, NaOH (0.5 M) was added to the column. The absorbance spectra of eluted fractions with NaOH were measured. Spectra of fractions 5, 7 (eluted with washing buffer at each pH) and 32 (eluted with NaOH) are shown in **b** for each pH 4.0, 7.0 and 12.6

shows the spectra of different fractions (5, 7 and 32) for samples prepared at pH 4.0, 7.0 and 12.6.

Imidazole interaction with Cb_5

Visible spectra of Cb_5 incubated at alkaline pH and imidazole effect

We analyzed the effect of imidazole as a potential ligand for the heme cavity, when this cavity is available. For other soluble hemoproteins, exogenous ligands have the ability to bind to the heme group by displacement of the native ligand, i.e., methionine in the case of Cyt *c* and Cyt c_2 [43, 44]. Therefore, imidazole binding to some hemoproteins produces a blueshift in the Soret region [45]. In the case of some Cb_5 mutants, the spectra are expected to change after addition of imidazole when it has been used for the same purpose [46].

To quantify the changes induced by imidazole on the protein, we measured the difference spectra of Cb_5 in the

presence and absence of imidazole, once the Soret band absorbance was stabilized (Fig. 4b). The Cb_5 difference spectra at pH 11.0, 11.5, 12.0, 12.5 and 13.0 are shown in Supp. Fig. S5. Each line corresponds to the following imidazole concentrations: 50, 100, 150, 200, 250, 300, 400 and 500 mM. At pH values below 12.5, the decrease of the Soret band was dependent upon imidazole concentration being this spectral change synchronized in time with the appearance of a band around 430–436 nm. Both events were dependent upon the imidazole concentration present in the assay (band changes are indicated by arrows). This effect was better observed when a difference spectrum was recorded (imidazole vs. no imidazole addition) at pH 11.5 (gray line) (Fig. 6a and Supp. Fig. S5). At pH 12.5 and pH values above, addition of imidazole induced an increase of the Soret band (maximum absorbance at 410-414 nm), as shown by the difference spectra of a sample incubated with imidazole vs no imidazole at pH 13.5 (Fig. 6a, black line and Figs. S5C, S5D and S5E). The absorbance increase at 414
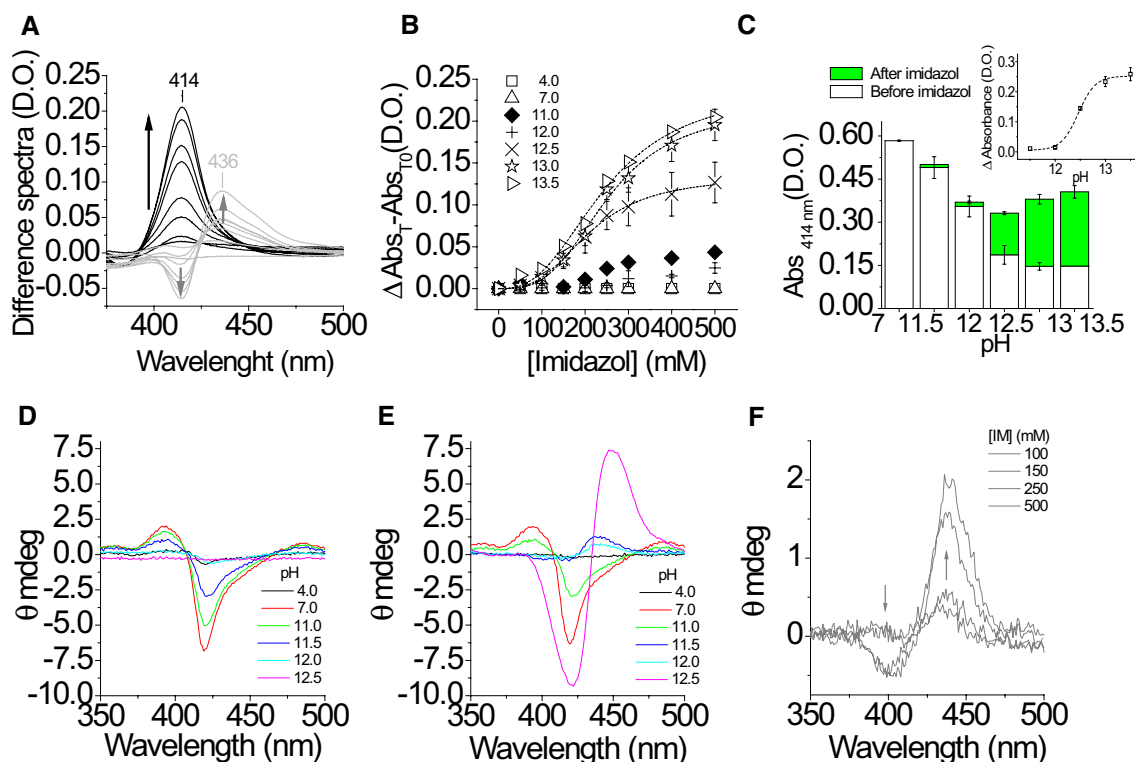
Fig. 6 Cb_5 spectral changes induced by imidazole. Difference spectra of samples incubated at pH Cb_5 11.5 and 13.5 in the presence of increasing imidazole concentrations with respect to absence is shown in **a**. After Cb_5 (50 µM) incubation in the buffer at each pH with time, Soret band loss was stabilized. Aliquots of dilute concentration (5 µM) in buffer were prepared at each pH with the imidazole concentration indicated in the figure. The absorbance increment dependence with imidazole concentration of samples associated with changes in the Soret band measured at 414 nm is shown in **b**. A plot of the Soret absorbance lost (gray bar) upon incubation of the sample

at each pH and the recovery of the Soret band induced by imidazole (green bar is shown in **c**). Inlet indicates the recovery of the absorbance by imidazole (500 mM) dependent on pH. Cb_5 Soret-CD spectra were measured as indicated in "Materials and methods" after incubation of the sample (15 µM) at each pH at the times when the Soret band loss was stabilized (**d**). The effect of imidazole (250 mM) on Cb_5 Soret-CD spectra was measured (**e**). The CD spectra of hemin (15 µM) complexed with increasing imidazole concentration at pH 12.0 is shown in **f** (arrows indicate the shift direction on hemin spectra incubated with increasing imidazole concentrations)

nm dependence upon imidazole concentration at different pH values is shown in Fig. 6b. The curves were fitted to the equation described in "Materials and methods". We calculated a K_d value for the imidazole complex with Cb_5 at each pH: 6.1 ± 1.1 μM, 3.0 ± 2.0 μM, 0.4 ± 0.2 μM, 0.5 ± 0.1 μM, 0.3 ± 0.2 μM and 2 ± 0.5 μM with Hill's coefficient (n) of: 1 ± 0.4, 1.2 ± 0.1, 1.6 ± 0.3, 1.6 ± 0.3, 1.7 ± 0.3, 1.2 ± 0.4 for pH 11.0, 11.5, 12.0 12.5, 13 and 13.5, respectively. The Soret band absorbance recovery induced by imidazole at saturating concentration (500 mM) (green bars) was compared to that found for Cb_5 after stabilization of the Soret band in time (white bars), at each pH before imidazole addition (Fig. 6c). The maximum absorbance recovery reached and induced by the presence of imidazole (500 mM) was also plotted as a dependence upon pH (Fig. 6c, inlet figure), allowing us to obtain a pK_a of 12.4 ± 0.1. To further discern between the interaction of imidazole to the heme ligated to Cb_5 or the free heme group at alkaline pH, we measured the Soret-CD spectra of free hemin and Cb_5, in the absence and presence of imidazole.

CD spectra of Cb_5 incubated at alkaline pH and imidazole effect

The Soret-CD spectra of Cb_5 was obtained at different pH values, 4.0, 7.0, 11.0, 11.5, 12.0 and 12.5 (Fig. 6d). At pH 7.0, the Soret-CD spectra have a negative band at 419 nm and a positive shoulder at 392 nm and 485 nm (red line).

At acid pH (4.0) (black line), the heme CD signal observed at pH 7.0 disappears suggesting a loss of the heme group chirality. At alkaline pH values, there was a pH-dependent disappearance of the Soret-CD bands described before (pH 11.0 and 11.5, green line and blue line, respectively). At pH 12.0 (light blue line), the Soret-CD signal almost disappears, and at pH 12.5 (pink line) there was no signal. Soret-CD spectra of Cb_5, in the presence of imidazole, were recorded at the same pH values and the results are shown in Fig. 6e. At pH 4.0, no signal and no changes induced by imidazole were found in the Soret-CD spectra. At pH 7.0, imidazole presence also did not affect the CD spectra. At pH 11.0, an intensity decrease of the heme-negative signal (at 419 nm) was observed with imidazole added to the assay. At pH 11.5 and 12.0, imidazole induced disappearance of the negative band at 419 nm and a positive band at 439 nm started to appear simultaneously. At pH 12.5, a strong symmetrical band appeared with a negative maximum at 419 nm and a strong positive band with a maximum at 440 nm.

To differentiate between the heme signal from the protein complexed with imidazole and that of the free hemin complexed with imidazole, CD spectra of the hemin–imidazole complex was measured at pH 12.0 (Fig. 6f). The CD spectra of a hemin solution 16 μM in the presence of imidazole

250 mM at this pH had a major positive band with a maximum at 440 nm with a minor negative shoulder at 401 nm.

Discussion

A structural and functional characterization of Cb_5 enzymatic activity was performed at alkaline and acid pH, based on previous reports showing a shift on the spin state induced by protein protonation and deprotonation [11, 12, 14]. We previously reported a peroxidase activity of Cb_5 dependent upon the acquisition of a non-native state by the protein at pH 12 (7). These results become highlighted when activities are compared between extreme pH values (pH 4.0 and 13.5) and show that protein reactivity is associated with the loss of the native protein structure. The oxygenase activity is higher at alkaline pH where the protein was still hexacoordinated than at acidic pH, where the heme group is mainly released (Figs. 1, 2 and 5) [7]. This effect was more clearly reflected when the peroxidase activity was measured and compared at both pH values: 4.0 and 12.0 (Table 1). The weak peroxidase activity at pH 4.0 vs. 12.0 is supported by measured enzymatic parameters: lower k_{cat} value for the peroxidase activity at acid pH (11 ± 1 ms^{-1}) in comparison to alkaline pH ($k_{cat} = 700 \pm 100$ ms^{-1}), as also denoted by the lower V_{max} 26 ± 5 nmoles/min/mg of Cb_5 with respect to 578 ± 41 nmoles/min/mg found at pH 12.0 [7], at saturating H_2O_2 concentration.

The results show that besides the low percentage of protein in a high spin state, other forces regulate this activity in alkaline media, since this parameter (spin state) does not sustain the differences on the peroxidase activity found at alkaline and acid pH by itself. Although a peroxidase activity has been shown for free hemin and some analogs, in alkaline media due to formation of oxo-iron porphyrin species [47, 48], this activity is lost upon formation of *bis*-coordinated bond with imidazole analogs [49]. Moreover, an effect induced by the possible hydroxide anion binding to the heme group at pH 12.0 was discarded, because the Cb_5 EPR spectra did not show any evidence for the interaction between hydroxide with the heme group [7]. To shed light on this behavior, a structural characterization of Cb_5 in correlation with activity measurements were performed at different pH values. ^{1}H-NMR data showed that at both acid (pH 4.0) and alkaline media (pH 12.0), there is disappearance of the heme resonances (Fig. 1a and Supp. Fig. S1) supporting a chemical exchange between different forms, which may reflect a spin equilibrium. Although we did not observe any additional resonance at higher frequencies (80–30 ppm) characteristics of a high spin state, above pH 11.0 the measured signal intensity decrease of the Cb_5 heme resonances (Supp. Fig. S1) are correlative with the heme spin alterations, observed by EPR at pH 12 [7].

At low pH values, the apparent decrease in intensity could be ascribed to a broadening beyond detection in the aggregated sample or an exchange phenomena between the native species and a minor fraction of the high spin species, that becomes dominant at lower pH values. Indeed, in a small protein containing a low spin, $S = 1/2$, heme ferric ion, a large fraction of resonances would experience pseudo-contact shifts and the loss of heme shall, therefore, cause chemical shift perturbations for all of these resonances.

In addition, our data support a stronger resilience of ferroCb_5 vs. ferriCb_5 heme resonances to suffer chemical shifts at alkaline pH values above 11, which correlates with the higher protein pK_a found by electrochemical methods for the reduced protein: $pK_{ox} = 11.6 \pm 0.1$ and $pK_{red} = 12.3 \pm 0.1$ for the oxidized and reduced protein, respectively (Supp. Fig. S2).

Our ^{15}N and ^1H NMR spectra (Fig. 1c) together with the far-UV CD spectra (Fig. 1d) indicates that the protein structure was already significantly affected at alkaline pH values. At pH 11.6, the reduced number of observed resonances in the HSQC spectra (Fig. 1c) can be ascribed to exchange with bulk water. Nevertheless, the peaks distribution suggest a different protein conformation with respect to neutral pH, as also supported by far-UV CD spectra, where the loss of secondary structure is already evident at pH 11 and pH 12. Noteworthy, the maximum protein unfolding was only achieved at pH 12.6, as shown by tryptophan fluorescence measurements (Fig. 3), with absence of a heme group release from the protein (Fig. 5). These results contrast with formation of distorted hexacoordinated Cb_5 species at pH 12, which have an intrinsic tryptophan fluorescence similar to that found in samples incubated at pH 7 [7]. Moreover, the tryptophan fluorescence increase found in samples incubated at pH values above 12 suggests that protein can get further unfolded, although not reaching those levels found in the Cb_5 sample incubated at pH 4 or by denaturalization using GDN 6 M (Fig. 3 and Supp. Fig. S4). Intrinsic tryptophan fluorescence of hemeproteins is very dependent on the quenching effect exerted by the heme group on the tryptophan residues (in this case a singular tryptophan residue present in the peptide chain). These results are in agreement with a heme group displacement in the heme cavity, that might be responsible for the detected protein alteration over the already distorted protein as shown by NMR, EPR and far-UV CD (Fig. 1 and Supp. Fig. S1), which affects the catalytic site leading to activity acquisition and ligand interaction with the heme iron (Figs. 2 and 6).

This effect can be correlated with Cb_5 tryptophan fluorescence increase detected in the sample incubated at acid pH values (Fig. 3) that also monitors the ligand accessibility to the heme iron, although for other reasons that does not happen at alkaline pH value, as it is the heme release from the peptide chain (Fig. 5). The effect found at acid pH values is coupled with protein aggregation present at pH 4, as measured by light scattering and the narrow distribution of the chemical shifts in the Cb_5 HSQC spectra at pH 4.8 (Fig. 1b, c), which suggest that the protein started getting denatured at acid pH. Precipitation of the sample at acid pH has also been described in other studies [50]. A reason for an immediate precipitation and aggregation of Cb_5 at pH values below 5.0 could be the collapse of the protein net charge from negative to positive values, since the isoelectric point of soluble Cb_5 is 4.3 [51]. This effect could be induced by glutamate ionization (pK_a 4.2 [52]), due to the high number of glutamic residues present in the protein as part of lobes holding the heme group [53]. In addition, the characteristic EPR high spin spectrum of Cb_5 at pH 4.0 (Fig. 1e, blue line) contrasts with the weak peroxidase activity found at this pH, in comparison to pH 12.0 [7]. Noteworthy, the oxygenase/peroxidase activity values found at both alkaline and acid pH values were higher than those found at neutral pH (absence of activity). The high activity found at alkaline media is also supported by the enhanced negative redox potential shifts observed at these pH values (Fig. 2d). The formal redox potential of Cb_5 found between pH 5.0 and 10.0, where no enzymatic activity was found, was very stable. The strong shift of the Cb_5 redox potential found from pH 11.0 to pH 13.0 (approx. −100 mV) allowed us to obtain an apparent pK_{ox} 11.6 ± 0.1 and pK_{red} 12.3 ± 0.1. A change in the redox potential could be associated with Cb_5 pentacoordination, since the protein was found to unfold at pH 12.6 and 4.0 (Fig. 3 and Supp. Fig. S4), also correlating with the highest oxygenase values present at both pH values and above pH 12.6 (Figs. 2 and 3). A trend toward negative values of the redox potential was also observed in acidic media below pH 6.0, in addition to the alkaline pH values, although sample aggregation did not allow us to obtain the conclusive data to calculate the apparent pK_{ox} and pK_{red} for the acid transition. Moreover, the different redox potentials observed between performed experiments, inside and outside the anaerobic chamber, in alkaline media, are in agreement with a possible O_2 binding to Cb_5, with a K_d of 1 ± 0.2 μM (Fig. 2e). This value was in the range of other K_d found for O_2 binding to other hemoproteins and in the low micromolar range [54]. This interaction is also expected to happen at acid media, although the small shift on Cb_5 redox potential at pH 4.0 did not allow us to accurately determine the effect of oxygen presence on the redox potential. The existence of O_2 binding to the protein correlates with the observed oxygenase activity found at this pH.

Protein autofluorescence emission (in the 300–360 nm wavelength range) recorded with a fixed excitation wavelength at 270 nm show a spectrum with two main contributors: tyrosine and tryptophan [25]. The intensity of these bands can be modulated by some factors, but the microenvironment modulating tyrosine and tryptophan autofluorescence and the distance between these residues (FRET)

make the discrimination between them not simple when a 270 nm excitation wavelength is used. Noteworthy, ionization of tyrosine is characterized by a redshift displacement of its maximum emission wavelength, allowing to track this residue ionization [25]. A role of tyrosine ionization has been described in the catalytic cycle of catalases, delocalizing the heme radical density on proximal weak ligands like tyrosinate or coupling the spin delocalization on this ionized amino acid residue [55, 56]. One of the three tyrosine residues of Cb_5 (Y34) is at less than 5 Angstroms from the heme group at neutral pH (Supp. Fig. S6), although we cannot discard the proximity of other tyrosine residues to the heme at alkaline pH. The presence of ionized tyrosine (pK_a 11.1 ± 0.1) also correlates with those pH values at which we started to observe an interaction of imidazole, before the measured unfolding by tryptophan fluorescence (pH 11.0–12.0) and the presence of a peroxidase activity associated with the hexacoordinated Cb_5 hemichrome at pH 12.0 [7]. Imidazole has been used to measure hemoprotein pentacoordination through the visible spectral shifts detected upon complex formation [45]. We found a differential effect induced by imidazole in alkaline media that was dependent upon pH. For Cb_5 prepared between pH 11.0 to pH 12.0, imidazole interaction with the protein induced a loss of the Soret band intensity. In contrast, imidazole induced an increase of the Soret band intensity above pH 12.0. Since above this pH we have measured, by the Cb_5 tryptophan fluorescence, a significant protein unfolding that leads to heme cavity opening (open Cb_5 conformation), our results point out that imidazole interaction with the protein is modulated by pH in the range 11 to 13.5. Thus, these results strongly suggest that imidazole interacts with the heme cavity, displacing the endogenous His ligand between pH values 11 and 12.1 (closed Cb_5 conformation), and directly with the heme cavity when the endogenous ligand was misligated, above pH 12.1 (open Cb_5 conformation).

In addition, when the protein was in the closed conformation, imidazole induced an increase of another band at 430–440 nm simultaneous to the decrease of the Soret band (Fig. 6). The band at 430–440 nm has been stated, in the bibliography, as the band for the *bis*-imidazole heme complex of free hemin. Analysis of the imidazole binding process (*n* value) allowed us to show that above pH 11.0, the interaction of one imidazole molecule induced some cooperativity (*n* more than 1) that could facilitate the release of the heme group from the cavity, as indicated by the appearance of this band at 430–440 nm. Therefore, our data support that at pH values below 12.5, imidazole destabilized the protein, inducing an enhanced solvent exposure of the heme group. CD and UV–visible experiments suggest that upon substrate ligation, the binding might facilitate the access to the catalytic site. Soret-CD spectra supported our results obtained with imidazole. Below pH 12.0, Cb_5 heme is influenced by

the peptide chain as shown by the chirality signal still present in the absence of imidazole. Upon addition of imidazole at those pH values, the loss of the band at 420 nm and appearance of the band a 440 nm on the CD spectra was time dependent and correlative with Cb_5 absorption data (disappearance of the absorption at 410 nm and appearance of the band at 435 nm). To assess that the absorption band found at 430–440 nm was associated with heme group release, we measured the CD spectra of hemin, in the presence of imidazole at pH 12.0. The results obtained corroborate the heme loss, due to the observation of a similar positive band at 440 nm in the CD spectra when complexed with imidazole (Fig. 6f). We demonstrated that the band at 430 nm in the visible spectra belongs to the free hemin *bis*-imidazole complex. The analysis of these data might also suggest that the catalytic site gets accessible to exogenous ligands in the closed conformation, when the protein structure is already distorted as shown by NMR, far-UV CD and EPR spectra. These results agree with the regulatory role of the surface-exposed areas located far from the catalytic site that regulate substrate affinity, turnover and drives some enzyme adaptation to low temperature through allosteric tuning [57].

In the open conformation above pH 12.5, imidazole induced the appearance of a strong band at 410 nm in the visible spectra as expected for the protein in a pentacoordinated state, allowing ligands like imidazole to interact with the heme group. Our Soret-CD spectra confirmed that imidazole added at these pH values induced a return of the chirality (previously lost by sample incubation in time).

To summarize, our results show a correlation between hemichrome formation and the low and high spin state transition of Cb_5 (closed and open conformation) in alkaline media, as supported in the competition assays with imidazole and unfolding measurements. The presence of exogenous ligands like imidazole would compete with the endogenous ligands (histidine residues) at alkaline pH (above pH 11). The use of imidazole to monitor an open and closed conformation in proteins has also been used for some CCP catalases and Cb_5 mutants [58]. The mechanism that we propose in terms of substrate accessibility to the Cb_5 catalytic site (heme), at these pH values, would not differ from that present in other similar hemoproteins such as cytoglobin [59], where the protein is hexacoordinated and becomes pentacoordinated upon ligand binding and explains the strong peroxidase activity found in these conditions. Once the pentacoordinated state is present or induced by ligand binding, hydrogen peroxide is expected to generate highly reactive radical species or associated signals to compound I and II supported by our previous data [7].

References

1. Rechetzki KF, Henneberg R, da Silva PH, do Nascimento AJ (2012) Rev Bras Hematol Hemoter 34:14–16
2. Percy MJ, McFerran NV, Lappin TR (2005) Blood Rev 19:61–68
3. Rifkind JM, Nagababu E, Ramasamy S, Ravi LB (2003) Redox Rep 8:234–237
4. Merlino A, Howes BD, Prisco G, Verde C, Smulevich G, Mazzarella L, Vergara A (2011) IUBMB Life 63:295–303
5. Peisach J, Mims WB (1977) Biochemistry 16:2795–2799
6. Lin YW, Wang J (2013) J Inorg Biochem 129:162–171
7. Samhan-Arias AK, Maia LB, Cordas CM, Moura I, Gutierrez-Merino C, Moura JJG (2018) Biochim Biophys Acta Proteins Proteom 1866:373–378
8. Vergara A, Franzese M, Merlino A, Bonomi G, Verde C, Giordano D, di Prisco G, Lee HC, Peisach J, Mazzarella L (2009) Biophys J 97:866–874
9. Rachmilewitz EA (1969) Ann N Y Acad Sci 165:171–184
10. Peisach J, Blumberg WE, Adler A (1973) Ann N Y Acad Sci 206:310–327
11. Bois-Poltoratsky R, Ehrenberg A (1967) Eur J Biochem 2:361–365
12. Ikeda M, Iizuka T, Takao H, Hacihara P (1974) Biochimica et Biophysica Acta (BBA). Protein Struct 336:15–24
13. Vergara A, Franzese M, Merlino A, Vitagliano L, Verde C, di Prisco G, Lee HC, Peisach J, Mazzarella L (2007) Biophys J 93:2822–2829
14. Vickery L, Nozawa T, Sauer K (1976) J Am Chem Soc 98:351–357
15. Avila L, Huang H-W, Rodríguez JC, Moënne-Loccoz P, Rivera M (2000) J Am Chem Soc 122:7618–7619
16. Rodríguez JC, Rivera M (1998) Biochemistry 37:13082–13090
17. Isom DG, Castaneda CA, Cannon BR, Garcia-Moreno B (2011) Proc Natl Acad Sci USA 108:5260–5265
18. Fitch CA, Platzer G, Okon M, Garcia-Moreno BE, McIntosh LP (2015) Protein Sci 24:752–761
19. Grimsley GR, Scholtz JM, Pace CN (2009) Protein Sci 18:247–251
20. Pundak S, Roche RS (1984) Biochemistry 23:1549–1555
21. Samhan-Arias AK, Almeida RM, Ramos S, Cordas CM, Moura I, Gutierrez-Merino C, Moura JJG (2018) Biochim Biophys Acta Bioenerg 1859:78–87
22. Keller RM, Wuthrich K (1980) Biochim Biophys Acta 621:204–217
23. La Mar GN, Burns PD, Jackson JT, Smith KM, Langry KC, Strittmatter P (1981) J Biol Chem 256:6075–6079
24. Samhan-Arias AK, Garcia-Bereguiain MA, Martin-Romero FJ, Gutierrez-Merino C (2006) J Fluoresc 16:393–401
25. Lakowicz JR (2006) Principles of fluorescence spectroscopy. Springer, New York
26. Nastri F, Lista L, Ringhieri P, Vitale R, Faiella M, Andreozzi C, Travascio P, Maglio O, Lombardi A, Pavone V (2011) Chemistry 17:4444–4453
27. Lloyd E, Ferrer JC, Funk WD, Mauk MR, Mauk AG (1994) Biochemistry 33:11432–11437
28. McLachlan SJ, La Mar GN, Burns PD, Smith KM, Langry KC (1986) Biochim Biophys Acta 874:274–284
29. McLachlan SJ, La Mar GN, Burns PD, Smith KM, Langry KC (1986) Biochim Biophys Acta 874:274–284
30. Slaughter SR, Williams CH Jr, Hultquist DE (1982) Biochim Biophys Acta 705:228–237
31. Gray FLV, Murai MJ, Grembecka J, Cierpicki T (2012) Protein Sci A Publ Protein Soc 21:1954–1960
32. Tomar SK, Knauer SH, Nandymazumdar M, Rosch P, Artsimovitch I (2013) Nucleic Acids Res 41:10077–10085
33. Mayor U, Günter Grossmann J, Foster NW, Freund SMV, Fersht AR (2003) J Mol Biol 333:977–991
34. Kitahara R, Okuno A, Kato M, Taniguchi Y, Yokoyama S, Akasaka K (2006) Magn Reson Chem 44:S108–S113
35. Peng HM, Auchus RJ (2014) Arch Biochem Biophys 541:53–60
36. Moura I, Pauleta SR, Moura JJ (2008) J Biol Inorg Chem 13:1185–1195
37. Field SJ, Roldan MD, Marritt SJ, Butt JN, Richardson DJ, Watmough NJ (2011) Biochim Biophys Acta (BBA) Bioenerg 1807:451–457
38. Cordas CM, Duarte AG, Moura JJ, Moura I (2013) Biochim Biophys Acta 1827:233–238
39. Katchalski E, Sela M (1953) J Am Chem Soc 75:5284–5289
40. Sela M, Katchalski E (1956) J Am Chem Soc 78:3986–3989
41. Schwans JP, Sunden F, Gonzalez A, Tsai Y, Herschlag D (2013) Biochemistry 52:7840–7855
42. Mrazova B, Martinkova M, Martinek V, Frei E, Stiborova M (2008) Interdiscip Toxicol 1:190–192
43. Dumortier C, Holt JM, Meyer TE, Cusanovich MA (1998) J Biol Chem 273:25647–25653
44. Ikeda-Saito M, Iizuka T (1975) Biochim Biophys Acta 393:335–342
45. Schejter A, Aviram I (1969) Biochemistry 8:149–153
46. Wang WH, Lu JX, Yao P, Xie Y, Huang ZX (2003) Protein Eng 16:1047–1054
47. Portsmouth D, Beal EA (1971) Eur J Biochem 19:479–487
48. Schugar HJ, Walling C, Jones RB, Gray HB (1967) J Am Chem Soc 89:3712–3720
49. Uno T, Takeda A, Shimabayashi S (1995) Inorg Chem 34:1599–1607
50. Moore CD, Al-Misky ON, Lecomte JT (1991) Biochemistry 30:8357–8365
51. Abe K, Sugita Y (1979) Eur J Biochem 101:423–428
52. Berg JM, Tymoczko JL, Stryer L, Stryer LB (2007) Biochemistry. In: Freeman WH (ed) Basingstoke. Palgrave, New York (distributor)
53. Gill DS, Roush DJ, Willson RC (1994) J Chromatogr A 684:55–63
54. Wittenberg JB (1966) J Biol Chem 241:104–114
55. Chuang WJ, Van Wart HE (1992) J Biol Chem 267:13293–13301
56. Vidossich P, Alfonso-Prieto M, Rovira C (2012) J Inorg Biochem 117:292–297
57. Saavedra HG, Wrabl JO, Anderson JA, Li J, Hilser VJ (2018) Nature 558:324–328
58. Erman JE, Chinchilla D, Studer J, Vitello LB (2015) Biochim Biophys Acta 1854:869–881
59. de Sanctis D, Dewilde S, Pesce A, Moens L, Ascenzi P, Hankeln T, Burmester T, Bolognesi M (2004) J Mol Biol 336:917–927